

Microstructure evolution of 7050 aluminum alloy during hot deformation

LI Jun-peng(李俊鹏), SHEN Jian(沈 健), YAN Xiao-dong(闫晓东),
MAO Bai-ping(毛柏平), YAN Liang-ming(闫亮明)

General Research Institute for Non-Ferrous Metals, Beijing 100088, China

Received 4 December 2008; accepted 27 March 2009

Abstract: Hot compression of 7050 aluminum alloy was performed on Gleeble 1500D thermo-mechanical simulator at 350 °C and 450 °C with a constant strain rate of 0.1 s^{-1} to different nominal strains of 0.1, 0.3 and 0.7. Microstructures of 7050 alloy under various compression conditions were observed by TEM to investigate the microstructure evolution process of the alloy deformed at various temperatures. The microstructure evolves from dislocation tangles to cell structure and subgrain structure when being deformed at 350 °C, of which dynamic recovery is the softening mechanism. However, continuous dynamic recrystallization (DRX) occurs during hot deformation at 450 °C, in which the main nucleation mechanisms of DRX are subgrain growth and subgrain coalescence rather than particle-stimulated nucleation (PSN).

Key words: microstructure evolution; dynamic recovery; dynamic recrystallization; hot deformation; 7050 alloy

1 Introduction

The softening (restoration) processes of recovery and recrystallization may occur during deformation at high temperatures. In this case, the phenomena are called dynamic recovery (DRV) and dynamic recrystallization (DRX) in order to distinguish them from the static annealing processes which occur during post-deformation in heat treatment. Dynamic recovery and dynamic recrystallization are important because they lower the flow stress of the material, thus enable it to be deformed more easily[1]. It has been long claimed that only dynamic recovery, i.e., dislocation rearrangement (repolygonization) and annihilation, took place to oppose strain hardening in high stacking fault energy (SFE) metals[1–3]. However, in recent years, DRX phenomena were found in pure Al, Al-Mg, and Al-Zn alloys; and these alloys usually undergo continuous (CDRX) rather than discontinuous (DDRX) dynamic recrystallization during high temperature deformation[2, 4–5].

7050 aluminum alloy, a typical Al-Zn-Mg-Cu series aluminum alloy, which belongs to precipitation-strengthened alloy, is widely used due to its high strength and low density[6]. Most researches on 7050 alloy are concentrated on the heat treatment process. So far, less research has been given to the microstructure evolution

process during high temperature deformation [6–8]. In this work, microstructure of 7050 alloy deformed to different strains at different temperatures under constant strain rate were analyzed with transmission electron microscope (TEM). Therefore, softening process occurring under different deformation conditions can be detected.

2 Experimental

The material selected for this investigation was semi-continuous casting 7050 alloy ingots from Southwest Aluminum Fabrication Plant, China, with a composition of Al-6.0Zn-2.20Mg-2.23Cu-0.1Mn-0.1Zr (mass fraction, %). The mean grain size is about 80 μm after heat treatment. Rastegaev specimens of $d_{10} \text{ mm} \times 15 \text{ mm}$ were obtained by mechanical processing, of which the axial direction is parallel to the short transverse direction of the ingot.

Hot compression tests were performed on Gleeble 1500D thermo-mechanical simulator at 350 and 450 °C with a constant strain rate of 0.1 s^{-1} . The specific strains were 0.1, 0.3 and 0.7. The experimental stress—strain curves under various deformation conditions were obtained.

The deformed specimens were water quenched after

compression to maintain the microstructures for TEM observations. The deformed specimens were then sectioned parallel to the axis, ground and electropolished. The misorientation and its distributions of deformed 7050 alloy with different strains were investigated by electron back-scattered diffractometry (EBSD) on the electropolished specimens. Thin foil TEM samples were prepared by cutting the longitudinal section of the deformed specimen using electrical-discharge machining. The discs were ground to a thickness of about 50 μm , then were subjected to twin-jet electro-polishing. TEM observations were made on a H800 transmission electron microscope operated at 160 kV.

3 Results

3.1 Stress—strain curves

The stress—strain curves of 7050 alloy deformed at 350 $^{\circ}\text{C}$ to nominal strains of 0.1, 0.3 and 0.7 are shown in Fig.1(a). Good fits of the three curves can be observed, and the similar result can be obtained when the alloy is deformed at 450 $^{\circ}\text{C}$. It is well-known that the stress and microstructure of the material have a reasonable one-to-one correspondence. Thus, the rules of microstructure evolution process for 7050 alloy can be obtained through the observation and analysis of the microstructures of the specimens deformed to various strains.

The strain—stress curves of 7050 alloy deformed to the same strain of 0.7 at different temperatures are shown in Fig.1(b). It can be seen clearly that the strain—stress curve of 7050 alloy deformed at 350 $^{\circ}\text{C}$ is typically characterized by a rise to a plateau followed by a constant flow stress, which is the feature of curves for DRV. This indicates that the main softening mechanism of 7050 alloy in this condition is DRV. However, the strain—stress curve of 7050 alloy deformed at 450 $^{\circ}\text{C}$ exhibits a single and smooth peak, followed by a slow

but obvious softening stage, which is quite different from that deformed at 350 $^{\circ}\text{C}$. It is reasonable to presume that the softening mechanism in this condition may be DRX.

3.2 Microstructures of 7050 alloy during hot deformation

Fig.2 shows the TEM bright field images of the microstructures of 7050 alloy deformed to various strains at 350 $^{\circ}\text{C}$. The microstructures of the alloy deformed to a strain of 0.1 at 350 $^{\circ}\text{C}$ are shown in Figs.2(a) and (b). The microstructure in Fig.2(a) shows the transformation from dislocation cell structure to subgrain structure. A tendency associated with the formation of subgrain structure appears from the TEM observation since the ‘cell walls’ become sharp to form the subgrain boundaries, which implies that the annihilation of dislocation within cells happens due to dislocation movement. Fig.2(b) shows the amplification of the central-upside area of Fig.2(a). A hexagonal twist boundary which is the consequence of DRV belonging to low angle boundary can be observed clearly. Fig.2(c) shows the microstructure of 7050 alloy deformed to a strain of 0.3 at 350 $^{\circ}\text{C}$. Subgrain structure with clear boundaries can be found obviously, which indicates that the evolution of cell structure to subgrain structure is finished. Fig.2(d) shows the microstructure of 7050 alloy deformed to a strain of 0.7 at 350 $^{\circ}\text{C}$. Well developed subgrains which are approximately equiaxed are the main feature of the microstructure at this situation. A large amount of dislocations in the subgrains can also be observed in Fig.2(c). The mean subgrain size in Fig.2(d) is about 1.5 μm , which is approximately the same with that in Fig.2(c). The subgrain boundaries are clear and the main misorientation between subgrain boundaries determined by EBSD measurement is about 3 $^{\circ}$.

TEM microstructures of 7050 alloys deformed to various strains at 450 $^{\circ}\text{C}$ are shown in Fig.3. Grain boundary maps and misorientation distribution maps of

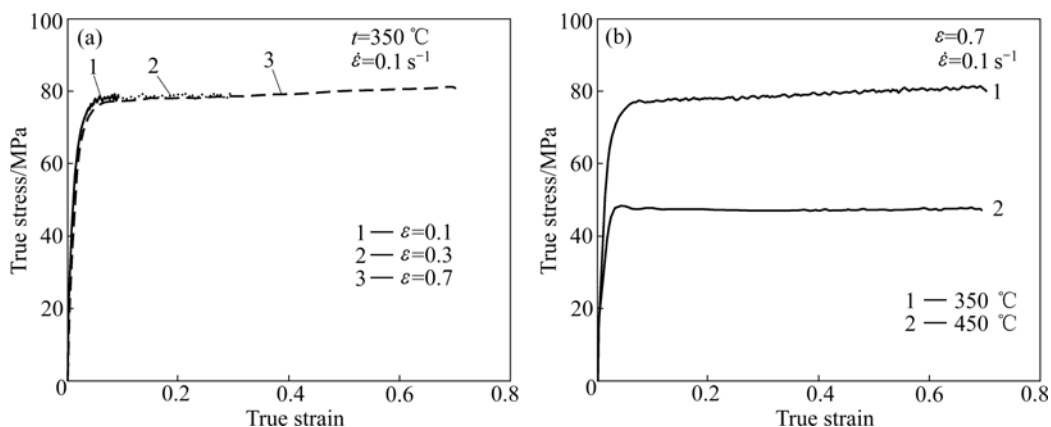


Fig.1 Stress—strain curves of 7050 alloy deformed under different conditions: (a) At 350 $^{\circ}\text{C}$ with various strains; (b) With strain of 0.7 at 350 and 450 $^{\circ}\text{C}$

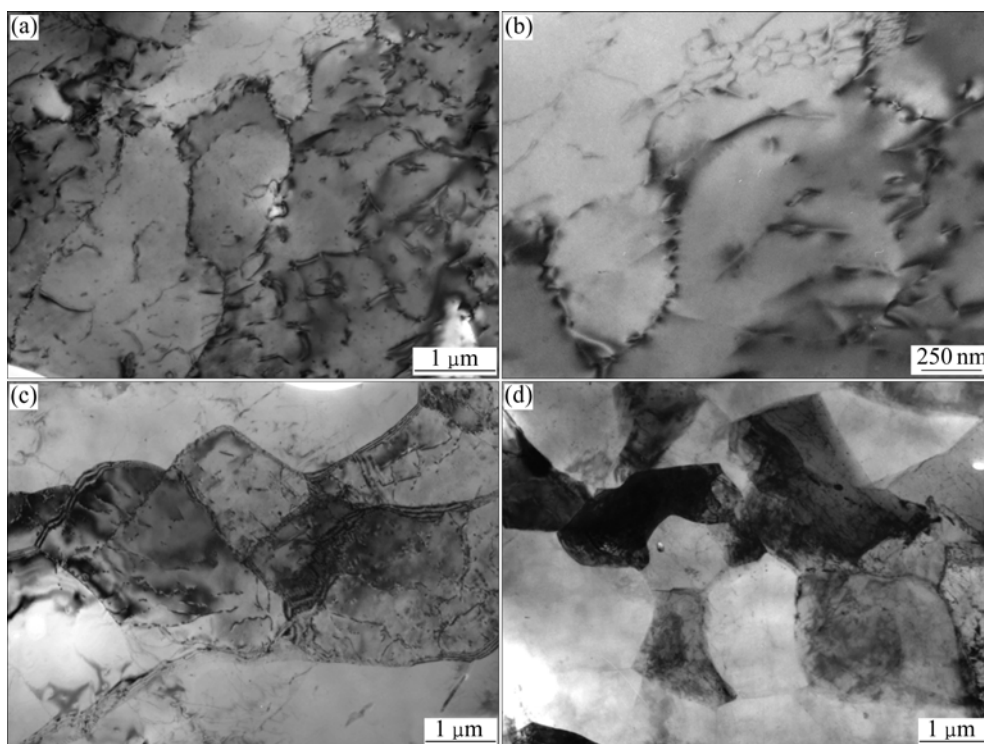


Fig.2 Microstructures of 7050 alloy deformed to various strains at 350 °C: (a) and (b) $\varepsilon=0.1$; (c) $\varepsilon=0.3$; (d) $\varepsilon=0.7$

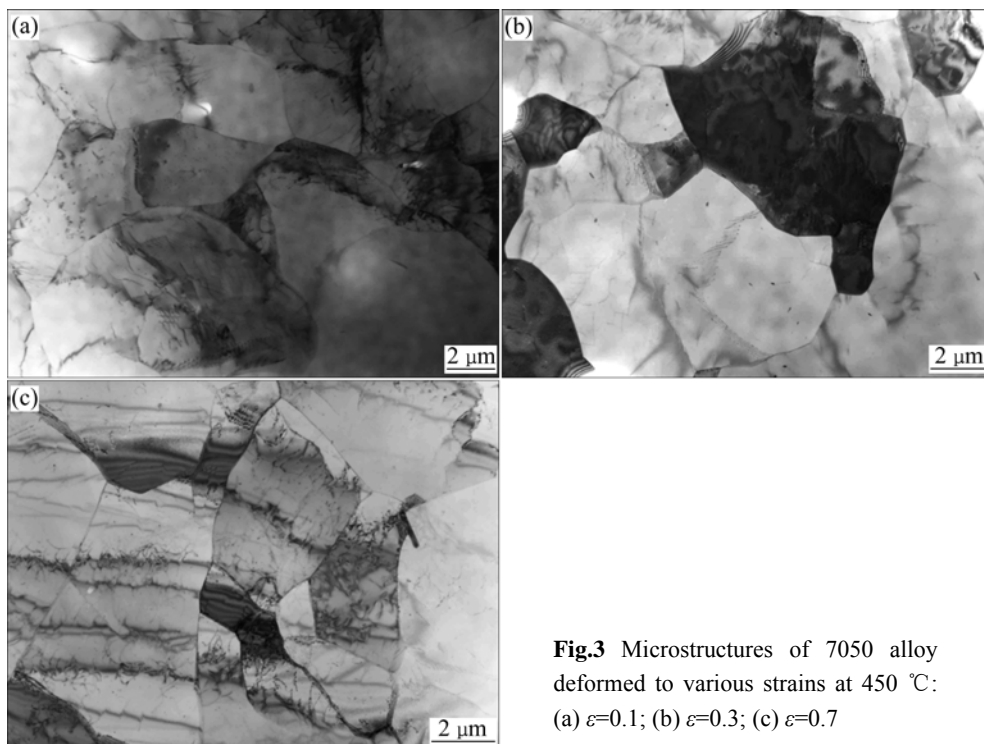


Fig.3 Microstructures of 7050 alloy deformed to various strains at 450 °C: (a) $\varepsilon=0.1$; (b) $\varepsilon=0.3$; (c) $\varepsilon=0.7$

7050 alloy deformed to various strains are shown in Fig.4. The microstructure of 7050 alloy deformed to a strain of 0.1 at 450 °C is shown in Fig.3(a), the main feature of which is the well developed subgrain structure. The subgrain boundaries are sharp but the misorientation between subgrains is small, about 1°–2°, as seen in Fig.4(a). The mean size of the subgrains in this condition

is about 3.5 μm , which is larger than that of the sample deformed at 350°C. When the specimen is deformed to a strain of 0.3 at 450 °C, as shown in Fig.3(b), the mean size of the subgrains is 6 μm , and the misorientation between subgrains becomes large, as shown in Fig.4(b), which shows a tendency that subgrains with medium misorientation ($> 5^\circ$) appears (marked by arrows in

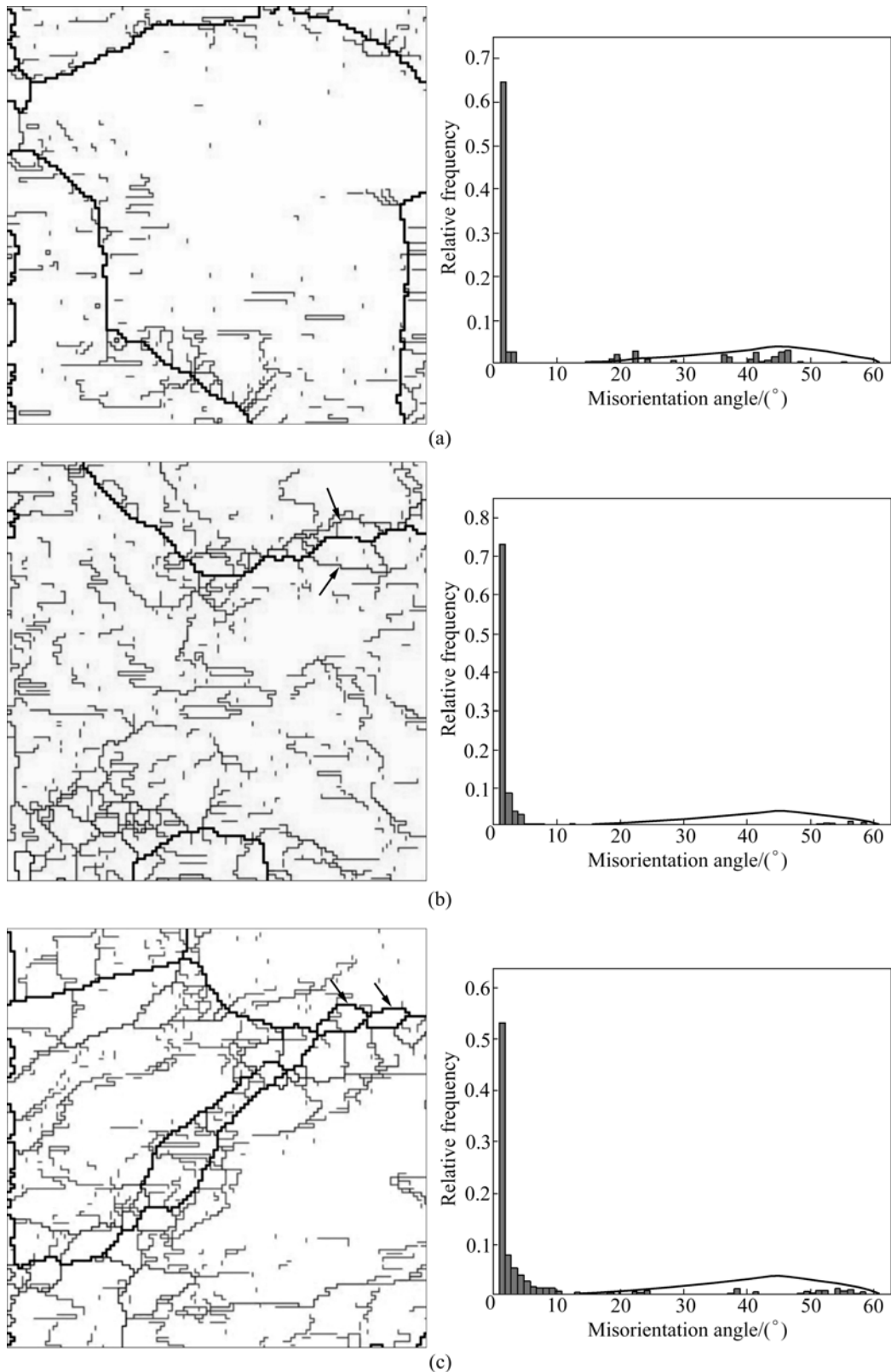


Fig.4 Grain boundary maps and corresponding misorientation angle distribution maps of 7050 alloy deformed to various strains at 450 °C: (a) $\varepsilon=0.1$; (b) $\varepsilon=0.3$; (c) $\varepsilon=0.7$

Fig.4(b)). Traces of subgrain coalescence and subgrain growth can be detected. Fig.3(c) shows the representative microstructure of 7050 alloy deformed to a strain of 0.7

at 450 °C, which presents a typical recrystallization structure. The grain boundaries are straight; some of the misorientations between subgrain boundaries are larger

than 15° (marked by arrows in Fig.4(c)); and subgrains of low dislocation density and some of high dislocation density can be detected. High-angle (subgrain) boundaries (HABs) existing on the original grain boundary can be observed clearly in the grain boundary map shown in Fig.4(c) (marked by arrows). The grains with HABs are about $12\ \mu\text{m}$ in size, since the mean original grain size is about $80\ \mu\text{m}$, and these grains are of the DRX structure characteristic. The ratio of high misorientation increases from the misorientation distribution map in Fig.4(c), which is another evidence of the occurrence of DRX.

4 Discussion

Generally, microstructure evolution during hot deformation is determined by strain hardening and dynamic softening processes which are two contradictory processes during hot working. Dislocation generation and intersection during plastic deformation lead to work hardening, while dynamic softening is mainly supplied by DRV and DRX[1, 3, 9–10].

As can be seen from the microstructures shown in Fig.2, when 7050 alloy is deformed at $350\ ^\circ\text{C}$, the microstructure evolves from dislocation tangles to cells and subgrain structure, in which the main softening mechanism is DRV.

It is generally accepted that during the initial stage of deformation, dislocation density rises rapidly due to strain hardening. Dislocations moves through slipping and gliding under the applied stress to form the pile-up of dislocations and dislocation locks. Therefore, the dislocations are tangled in this stage. Gradually, the dislocation density in regions close to tangled area is somewhat lower and the dislocation cell structure appears[9–10]. In metals of high stacking fault energy such as aluminum and its alloys, climbing is rapid, so significant dynamic recovery may occur. There are two primary processes, that is, the dislocation annihilation and dislocation rearrangement into lower energy configurations[3, 11–13]. As shown in Fig.2(a), the dislocation cells gradually evolve to form subgrain structure through the movement of mobile dislocation to cell boundaries and annihilation of dislocations in the cell boundaries. As dynamic recovery happens, the stored energy of material is lowered by dislocation movement to form the low energy boundaries, as shown in Fig.2(b). Finally, the subgrain structure of low-angle (subgrain) boundaries (LABs) forms.

The misorientation of the subgrain boundaries increases to about 3° and then remains constant[3, 9–11]. The processes of work hardening and recovery lead to the continuous formation and dissolution of LABs; and the subgrain structure appears to achieve a steady state

with a constant mean subgrain size and a constant dislocation density within the subgrains. It is generally accepted that the true stress during hot deformation is determined by the subgrain size, misorientation between subgrains and the dislocation density in subgrains. Therefore, it is reasonable that the stresses of 7050 alloy deformed to strains of 0.3 and 0.7 are approximately the same due to the similar mean subgrain size and main misorientation, as seen in Figs.2(c) and (d).

DRX occurs during the hot deformation of 7050 alloy at $450\ ^\circ\text{C}$ based on the observation of Fig. 3 and Fig.4. It is clear that 7050 alloy deformed at $450\ ^\circ\text{C}$ undergoes CDRX from the observation of stress—strain curve since there is no board peak on the curve. Moreover, the main misorientation raises gradually during hot compression.

With regard to the DRX nucleation mechanism, there is evidence that a process similar to the particle-stimulated nucleation (PSN) of recrystallization on static annealing of alloys containing large particles may occur during high temperature deformation[2, 5, 14–16]. The stable $\eta(\text{MgZn}_2)$ and $S(\text{Al}_2\text{CuMg})$ phases with the size of about $2\ \mu\text{m}$ precipitate during the heat treatment[7–8]. It seems reasonable that the DRX nucleation mechanism for 7050 alloy during hot deformation is PSN. However, there is little evidence for particle-stimulated dynamic recrystallization in aluminum alloys. HUMPHREYS and KALU found small highly-misoriented grains adjacent to large second-phase particles, but these grains were generally of a similar size to the subgrains remote from the particles and there was little evidence of their growth [2, 5]. It is likely that such nuclei are formed by dynamic recovery of the misoriented subgrains during deformation, but the stored energy of the matrix is too low to allow those nuclei to grow. Particle-stimulated dynamic recrystallization will only be possible if dislocations accumulate at the particles during deformation. This will occur for larger particles at lower temperatures and higher strain rates. Through the TEM observation of microstructures for 7050 alloy deformed at $450\ ^\circ\text{C}$, no high-angle (subgrain) boundaries (HABs) are detected adjacent to the η phase. Therefore, the DRX nucleation mechanism for 7050 alloy deformed at 450°C is not PSN.

Through the observations of microstructures of 7050 alloys deformed at $450\ ^\circ\text{C}$ to various strains, subgrain growth by rotation and coalescence is the reasonable nucleation mechanism. Evidence of subgrain growth by rotation can be observed in Fig.3(b). Subgrains may rotate by boundary diffusion processes until adjacent subgrains are of similar orientation. The two subgrains involved will then coalesce into one larger subgrain with little boundary migration. The subgrain in Fig.3(b) shows the trace of subgrain growth by rotation

and coalescence, which also exists in the adjacent subgrain. After the subgrain growth, the size and misorientation with adjacent subgrains increase, which can enhance the mobility of the subgrain. Therefore, the growth of subgrains is further promoted, and the misorientation of grown subgrains will increase gradually. When a critical value of the misorientation angle is reached, the microstructure contains subgrain and grain structures, entirely delimited by HABs and LABs. Then, the nucleation process for DRX is completed, as seen in Fig.4(c), and grains with HABs emerge.

5 Conclusions

1) When 7050 alloy is deformed at 350 °C, the microstructure evolves from dislocation tangles to cells and subgrain, in which the main softening mechanism is DRV. The mean subgrain size and misorientation between subgrains of 7050 alloy remain constant after being deformed to a strain of 0.3.

2) While 7050 alloy is deformed at 450 °C, recrystallization grains of 12 μm in size can be observed, which indicates that continuous dynamic recrystallization occurs during the hot deformation, and the main nucleation mechanism is subgrain growth and coalescence rather than particle-simulated nucleation.

References

- [1] HUMPHREYS F J, HATHERLY M. Recrystallization and related annealing phenomena [M]. Oxford: Pergamon Press, 2004. 169–210.
- [2] DOHERTY R D, HUGHES D A, HUMPHREYS F J, JONAS J J, JUUL JENSEN D, KASSNER M E, KING W E, McNELLEY T R, McQUEEN H J, ROLLETT A D. Current issues in recrystallization: A review [J]. *Materials Science and Engineering A*, 1997, 238: 219–274.
- [3] KOCKS U F, MECKING H. Physics and phenomenology of strain hardening: the FCC case [J]. *Progress in Materials Sciences*, 2003, 48: 171–273.
- [4] YAMAGATA H, OHUCHIDA Y, SAITO N, OTSUKA M. Nucleation of new grains during discontinuous dynamic recrystallization of 99.998 mass% aluminum at 453 K [J]. *Scripta Materialia*, 2001, 45: 1055–1061.
- [5] McQUEEN H J. Development of dynamic recrystallization theory [J]. *Materials Science and Engineering A*, 2004, 387/389: 203–208.
- [6] MUKHOPADHYAY A K. High strength aluminum alloys for structural application [J]. *Metals Materials and Processes*, 2007, 119(1): 1–26.
- [7] ROBSON J D, PRANGNELL P B. Modelling Al₃Zr dispersoid precipitation in multi-component aluminium alloys [J]. *Materials Science and Engineering A*, 2003, 352(1/2): 240–250.
- [8] ROBSON J D. Micro-structural evolution in aluminum alloy 7050 during processing [J]. *Materials Science and Engineering A*, 2004, 382: 112–121.
- [9] NES E, MARTHINSEN K, BRECHET Y. On the mechanisms of dynamic recovery [J]. *Scripta Materialia*, 2002, 47: 607–611.
- [10] NES E, PETTERSEN T, MARTHINSEN K. On the mechanisms of work hardening and flow-stress saturation [J]. *Scripta Materialia*, 2000, 43: 55–62.
- [11] NES E, MARTHINSEN K, RUNNING B. Modeling the evolution in microstructure and properties during processing of aluminum alloys [J]. *Journal of Materials Processing Technology*, 2001, 117: 333–340.
- [12] SHERCLIFF, LOVATT A M, JUUL JENSEN D, BEYNON J H. Modeling of microstructure evolution in hot deformation [J]. *Philosophical Transactions: Mathematical, Physical and Engineering Sciences*, 1999, 357(1756): 1621–1643.
- [13] SELLARS C M. Modelling micro-structural development during hot rolling [J]. *Material Science and Technology*, 1990, 16(11): 1072–1078.
- [14] McQUEEN H J, KASSNER M E. Comments on ‘a model of continuous dynamic recrystallization’ proposed for aluminum [J]. *Scripta Materialia*, 2004, 51: 461–465.
- [15] KASSNER M E, BARRABES S R. New developments in geometric dynamic recrystallization [J]. *Materials Science and Engineering A*, 2005, 410/411: 152–155.
- [16] CHEN Hui-qin, CAO Chun-xiao, GUO Ling, LIN Hai. Hot deformation mechanism and microstructure evolution of TC11 titanium alloy in β field [J]. *Transactions of Nonferrous Metals Society of China*, 2008, 18(5): 1021–1027.

(Edited by YANG Bing)